Gating kinetics of Batrachotoxin-modified Na^+ channels in the squid giant axon

Voltage and temperature effects

Ana M. Correa,*‡ Francisco Bezanilla,*‡ and Ramón Latorre‡§

*Department of Physiology, Ahmanson Laboratory of Neurobiology and Jerry Lewis Neuromuscular Research Center, University of California, Los Angeles, California 90024; ‡The Marine Biological Laboratory, Woods Hole, Massachusetts, 02543; and §Departamento de Biología, Facultad de Ciencias, Universidad de Chile, Santiago, Chile, and Centro de Estudios Científicos de Santiago, Santiago, Chile

ABSTRACT The gating kinetics of batrachotoxin-modified Na^+ channels were studied in outside-out patches of axolemma from the squid giant axon by means of the cut-open axon technique. Single channel kinetics were characterized at different membrane voltages and temperatures. The probability of channel opening (P_o) as a function of voltage was well described by a Boltzmann distribution with an equivalent number of gating particles of 3.58. The voltage at which the channel was open 50% of the time was a function of [Na^+] and temperature. A decrease in the internal [Na^+] induced a shift to the right of the P_o vs. V curve, suggesting the presence of an integral negative fixed charge near the activation gate. An increase in temperature decreased P_o, indicating a stabilization of the closed configuration of the channel and also a decrease in entropy upon channel opening. Probability density analysis of dwell times in the closed and open states of the channel at 0°C revealed the presence of three closed and three open states. The slowest open kinetic component constituted only a small fraction of the total number of transitions and became negligible at voltages > -65 mV. Adjacent interval analysis showed that there is no correlation in the duration of successive open and closed events. Consistent with this analysis, maximum likelihood estimation of the rate constants for nine different single-channel models produced a preferred model (model 1) having a linear sequence of closed states and two open states emerging from the last closed state. The effect of temperature on the rate constants of model 1 was studied. An increase in temperature increased all rate constants; the shift in P_o would be the result of an increase in the closing rates predominant over the change in the opening rates. The temperature study also provided the basis for building an energy diagram for the transitions between channel states.

INTRODUCTION

Batrachotoxin (BTX), a toxin produced by the Colombian frogs of the genera *Phyllobates,* in particular *P. aurotaenia* (Daly et al., 1965; Daly et al., 1987), is able to induce profound changes in the behavior of nerve and muscle Na^+ channels (Daly and Witkop, 1971). Batrachotoxin shifts the voltage activation curve towards hyperpolarized voltages by ~50 mV (Albuquerque et al., 1971, 1973; Khodorov and Revenko, 1979; Huang et al., 1979, 1982; French et al., 1986a,b), suppresses fast and slow inactivation (Khodorov and Revenko, 1979; Huang et al., 1982; French et al., 1986a,b; Tanguy and Yeh, 1988; but see also, Huang et al., 1987), and increases the duration of Na^+ channel open events by more than one order of magnitude (Quandt and Narahashi, 1982). Moreover, BTX decreases channel conductance by ~50% and modifies ion selectivity (Quandt and Narahashi, 1982; Correa et al., 1991; Huang et al., 1982; Hille, 1984; Khodorov, 1985).

Despite the fact that ion permeation through the BTX-modified channel has received much attention (Moczydlowski et al., 1984; French et al., 1986a; Green et al., 1987; Garber, 1988; Behrens et al., 1989; Correa et al., 1991) detailed reports on channel gating kinetics are scarce. In this regard, the studies done both in neuroblastoma cells (Huang et al., 1984) and in lipid bilayers (Keller et al., 1986; French et al., 1986b; Behrens et al., 1989; Keller et al., 1990) agree in that gating kinetic models for the BTX-modified channel contain several closed states and one open state with no correlation in the durations of successive opening and closing events. The observation that only one open state can be discerned for the BTX-modified channel is puzzling because it would imply that BTX is stabilizing the open state already present in the absence of the toxin besides removing the fast and slow inactivation processes. A second possibility is that BTX is actually "creating" a new long lived open state and that normal openings of the channel have not been observed in previous studies because they were beyond the time resolution of the current measuring systems. In this regard, it is important to point out here that a different kinetic model for the squid axon BTX-modified channel was proposed by Tanguy and Yeh (1988) on the basis of their gating current measurements. Batrachotoxin, in contrast to other agents able to remove fast inactivation (e.g., pronase; Armstrong et al., 1973; Rojas and Rudy, 1976), removes Na^+ channel inactivation without suppressing charge immobilization. This led Tanguy and Yeh (1988) to propose that BTX is binding to the inactivation gate receptor without fully occluding the channel. This, in

0006-3495/92/05/1332/21 $2.00

kinetic terms, is equivalent to transforming the open-inactivated state into an open state. Therefore, adopting the model posed by Tanguy and Yeh (1988) for the BTX-modified channel, two open states are expected. It is clear that kinetic models, like those proposed for the BTX-modified Na^+ channel in neuroblastoma cells (Huang et al., 1984) and from different membrane sources incorporated into planar bilayers (Keller et al., 1986, 1990; French et al., 1986b; Behrens et al., 1989) used to account for the single-channel data, can not predict that charge immobilization be left intact by BTX as is the case in the squid Na^+ channel.

In this report, we study the gating kinetics of single squid axon BTX-modified Na^+ channels at different voltages and temperatures using the cut-open axon technique (Llano et al., 1988; Bezanilla and Vandenberg, 1990). The advantage of using this preparation to perform this kind of studies is twofold. First, it allows improvement in the time resolution compared with that possible when using planar lipid bilayers. In the latter case, the large capacitance severely limits the frequency of channel gating that can be monitored. Second, the changes induced by BTX in the kinetics of the macroscopic and gating currents of the squid sodium channel have been well characterized (Tanguy and Yeh, 1988, 1991). Since kinetic models extracted from single channel recordings must be consistent with the macroscopic data, the number of plausible models is immediately restricted.

Our study shows that the squid axon BTX-modified Na^+ channel has several closed and at least three open states. Adjacent interval and maximum likelihood analyses (McManus et al., 1985; Blatz and Magleby, 1989; Horn and Lange, 1983; Horn and Vandenberg, 1984) allowed us to reject several of the possible models, to perform a statistical comparison of models, and to estimate the rate constants of the transitions among states. We found that the preferred single-channel model has a linear sequence of closed states, and from the last closed state two open states are populated. Moreover, from the temperature dependence of the rate constants of the preferred model, we have derived a free energy diagram profile for the transitions of the channel between its kinetic states. Preliminary accounts of these results have been presented (Correa and Bezanilla, 1988; Correa et al., 1989).

MATERIALS AND METHODS

Squid axon preparation

The giant axon of the squid *Loligo pealei* was used for these experiments. The procedure to patch clamp the cut-open axon has been described in detail previously (Bezanilla, 1987; Bezanilla and Vandenberg, 1990; Llano et al., 1988). What follows is a summarized account of the technique. A segment of axon of ~1 cm in length, well cleaned of connective tissue, was pinned to the Sylgard-covered bottom of the experimental chamber. The axon was then cut longitudinally with microscissors under artificial seawater (0 K^+ ASW) containing (in mM) 440 NaCl, 50 $MgCl_2$, 10 $CaCl_2$, 10 Hepes-Na, pH 7.6. After 2 to 5 min the axonal sheet was perfused with ASW in order to wash out as much of the axoplasm as possible. All the experiments reported here were done using the excised outside-out configuration of the patch clamp technique (Hamill et al., 1981). This configuration was achieved by moving the patch pipette close to the internal surface of the membrane, applying slight suction, and then withdrawing the pipette from the axonal sheet. The external solution was 540 NaCl and 10 Hepes-Na, pH 7.6. The pipette solution was either "530 Na", which contained 500 Na-glutamate, 10 NaCl, 20 NaF, 10 Hepes-Na, pH 7.3, "50 Na", which contained 125 Cs-glutamate, 20 CsF, 40 Na-glutamate, 10 NaCl, 5 Cs-EGTA, 10 Hepes-Cs, 470 sucrose, pH 7.3, or "514 Na", which was "530 Na" diluted 4%. The convention *external//internal* has been used in reference to the composition of the solutions for each experiment. Patch pipettes were fabricated from Corning 7040 or 7052 glass, coated with Sylgard, and had resistances in the recording solution of 4–10 Mohm. The temperature of the experimental chamber was modified using Peltier units (LLano et al., 1988).

Na^+ channel modification by BTX

Channels were modified by adding BTX to a final concentration of 0.2 μM. The modification of channels did not depend on which side the toxin was added to; in the majority of the experiments BTX was added to the pipette solution. It was found that the process of BTX modification of Na^+ channels could be accelerated by holding the patch at hyperpolarized voltages and then applying depolarizing voltage pulses for short periods of time. For more details regarding this point see Correa et al. (1991), also Tanguy and Yeh (1991). In addition, channels can be modified more rapidly by transiently raising the temperature of the bath to 15°C. As found by Correa et al. (1991), despite the fact that patches usually contained several unmodified Na^+ channels, it was common to find only one modified by BTX. Only patches containing a single BTX-modified Na^+ channel were used in this study.

Data acquisition and analysis

The methodology for pulse generation and data acquisition has been described in detail by Llano et al. (1988). Single-channel currents were stored on a digital tape (Bezanilla, 1985) for subsequent transfer to a digital computer for analysis. Before analysis all records were filtered with a bandwidth of 600 to 1,200 Hz by an eight-pole Bessel filter and were digitized at 50-μs sample intervals. Since in most patches unmodified channels coexisted with BTX-modified Na^+ channels (Correa et al., 1991), extreme care was taken in choosing BTX-modified single-channel records preferentially free of contaminant activity of unmodified channels. This was achieved by careful visual inspection of the recordings and by appropriate filtering. 700 Hz was found to be the best compromise between a reasonable time resolution for single channel analysis, a good separation of events from noise peaks, and minimal contamination by normal Na^+ channel openings. For the single channel records analyzed, contamination was negligible in the voltage range between −90 to −70 because unmodified channels are normally closed at these voltages. At more positive potentials, where the open probability of BTX-modified channels is large, most openings of normal Na^+ channels would appear on top of BTX-modified Na^+ channel openings, and therefore, did not interfere with event detection. At these same potentials, reopenings of normal channels originating from the closed level were rare because the

normal channel is for the most part inactivated. P_o was calculated by dividing the time the channel dwells in the open state by the total time of the current record at any given potential. It was found that in a small percentage of the records gating activity had sudden shifts of the probability of opening. For all the records analyzed here, P_o stability was carefully checked by dividing the single-channel record in partial records of 200 transitions each and estimating P_o during these partial records. The 50%-threshold-crossing technique was used for estimating event durations and for obtaining "idealized" records (Colquhoun and Sigworth, 1983). The durations of the open and closed states were corrected for filtering and dead time as described by Colquhoun and Sigworth (1983). Open and closed dwell time histograms, as logarithmic-binned data (Sigworth and Sine, 1987), were fitted by a sum of exponential probability density functions using maximum likelihood.

Adjacent interval analysis. The relationship between the durations of adjacent closed and open intervals was obtained using the method described by McManus et al. (1985) and by Blatz and Magleby (1989). This analysis makes an average of the duration of all the open events that accompany a closed event of a given length. In practice, the stored sequential data were searched for closed intervals whose duration fell in a series of specified ranges (conditioning open or closed interval) and the mean duration of open (or closed) intervals that occurred immediately before and after the conditioning interval was calculated. The mean of the open (closed) events adjacent to a given closed (open) interval was plotted against the central value of the conditioning closed (open) interval.

Maximum likelihood estimation of rate constants. The rate constants of a particular kinetic model for the BTX-modified Na^+ channel were fitted using the maximum likelihood procedure as described by Horn and Lange (1983) and Horn and Vandenberg (1984). The computer program used in this analysis was kindly provided by Dr. Richard Horn (Roche Institute, Nutley, NJ) and included dead time correction following the method of Roux and Sauve (1985). Parameters were estimated and likelihood surface searched to obtain the maximum log (likelihood) using a variable metric method algorithm kindly provided by Dr. Kenneth Lange (University of California at Los Angeles). Standard errors were obtained from the covariance matrix which is obtained during the estimation of the rate constants. Six sets of single-channel data obtained at 0°C were idealized with the 50% threshold method. The data sets were obtained at −90, −80, −70, −65, −60, and −50 mV. Models examined were linear, branched, or cyclic Markovian kinetic models. In the case of cyclic models, the nonindependent rate constants were determined using the principle of detailed balance, which demands that the product of the rate constants around a cycle in the clockwise direction must be equal to the product of the rate constants in the opposite direction. Models with five states and up to nine independent rate constants were used in model testing. The estimation of all eight parameters for ~6,000 transitions using dead time correction required about 2 h of computer time using an i-860-based microprocessor (Microway Inc., Kingston, MA). Models were first tested without dead time correction. The convergence to the maximum was not always confirmed for all voltages.

One important criterion to accept a model, regardless of the likelihood value, was how well it predicted dwell time distributions of the experimental data. We found that models fitted without dead time correction made very poor predictions of the properties of the experimental data; therefore, we tested all the models with the data set corrected for filtering and 0.25 ms of dead time before being processed by the maximum likelihood rate estimating program. The use of dead time correction made the convergence more difficult as revealed by many cases in which the covariance matrix and the asymptotic standard error could not be calculated. In the convergence column of Table 2, a plus sign indicates that the covariance matrix of the fitted parameters could be computed at all voltages and a minus sign indicates that this computation failed in one or more of the voltages tested. It is interesting to note here that without dead time correction all models, except cyclic models, had converged.

For a general comparison between models (nested and non-nested) Akaike's asymptotic information criterion (*AIC*) was used to rank models (Akaike, 1974; Horn and Vandenberg, 1984):

$$AIC = 2[(\text{number of parameters}) \times (\text{number of voltages}) - \log(\text{likelihood})].$$

The model with the lowest *AIC* rank is considered best. This ranking provided a method to compare models that could not be evaluated with likelihood ratios.

Once the most probable kinetic model at 0°C was identified, rate constants for this model were estimated at six different voltages for 3.3°C and at five different voltages for 8.5 and 14.3°C using the same procedure.

Estimation of valence and chemical free energy. When the logarithm of the rates for the transitions between states are fitted to a linear function of voltage, the slope gives the valence times the fraction of the electrical field sensed by the gating charges and the intercept gives the chemical free energy change ΔG for such transition. In practice, the fit at the different temperatures was done by minimization of the following double sum,

$$\sum_{j=1}^{M}\sum_{i=1}^{n_j}[y_{ij} - (\ln\frac{kT_j}{h} - \frac{\Delta G}{RT_j} - \frac{zF}{RT_j}V_i)]^2, \quad (1)$$

assuming that the valence is not affected by temperature and where y_{ij} is the logarithm of the experimental rate (or time constant), where the index i refers to each data point and the index j to each temperature, n_j is the total number of experimental points at temperature T_i, and M is the total number of temperature values taken. T is the absolute temperature, k is the Boltzmann constant, h the Plank constant, ΔG the free energy change, R the gas constant, z the apparent valence, and V the voltage.

RESULTS

Equilibrium behavior at different temperatures

Fig. 1 *A* illustrates typical current records taken at the indicated voltages and obtained from an outside-out patch containing a single BTX-modified Na^+ channel at 4°C. The channel remains open most of the time at voltages positive to −60 mV, it is open 50% of the time at −80 mV, and dwells mainly in the closed state when the voltage is made more negative than −90 mV. Fig. 1 *B* shows the probability of opening, P_o, as a function of the applied voltage for the experiment illustrated in Fig. 1 *A*. The solid line is the fit of the data to a double Boltzmann distribution and the dashed line is the fit to a single Boltzmann distribution. The double Boltzmann gave a better fit to the data indicating the presence of more than one closed state. The voltage dependence of the BTX-modified channel changed

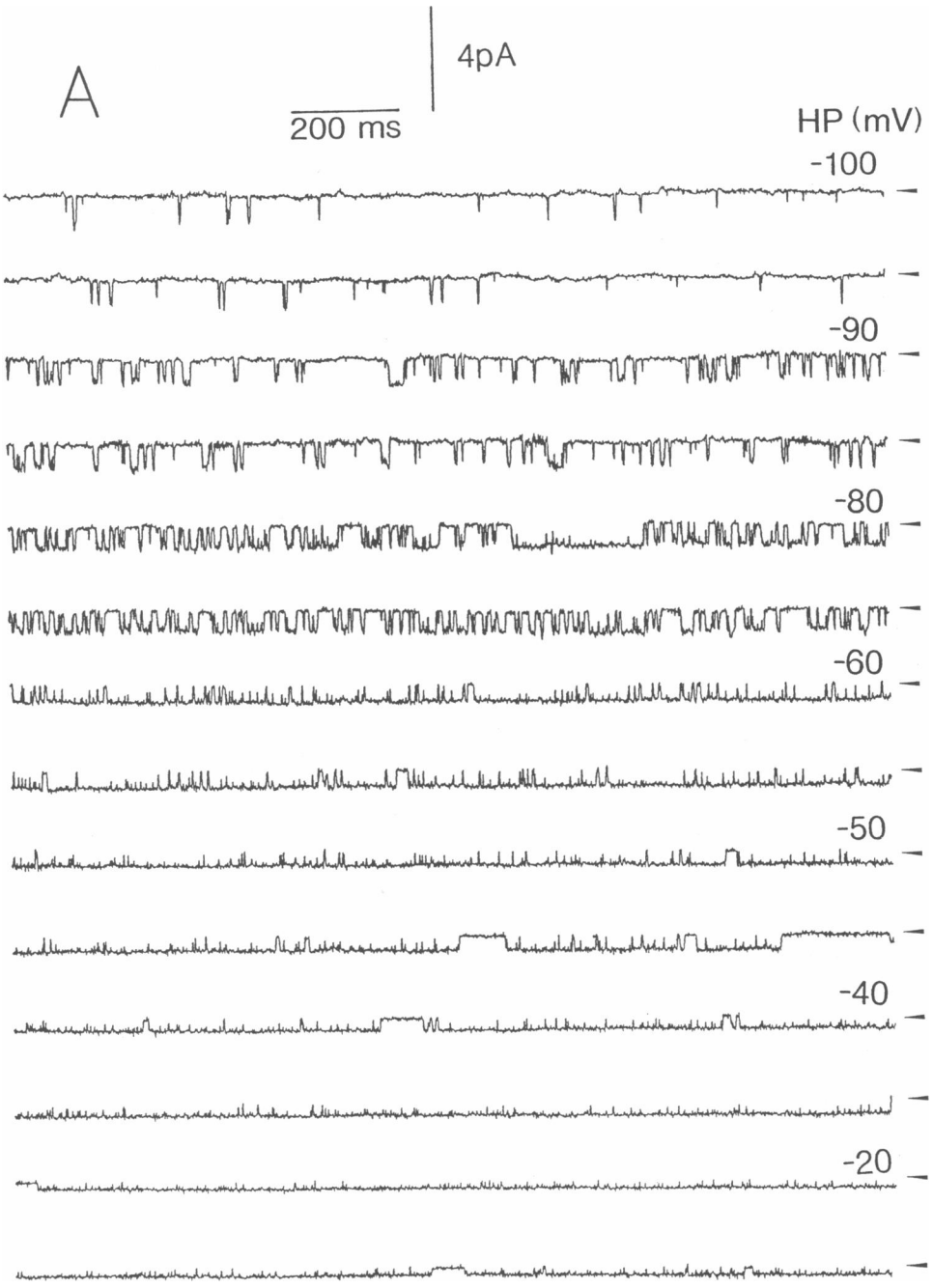

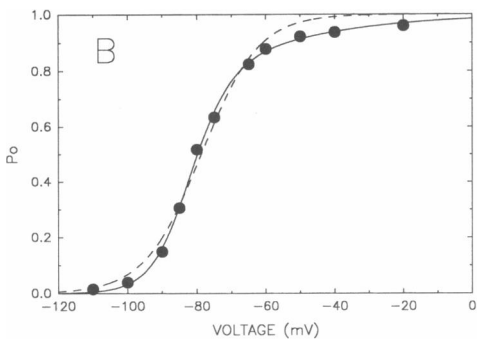

FIGURE 1 (*A*) Current records of a single squid axon BTX-modified Na^+ channel at different holding voltages. The records were obtained in an outside-out patch. Only one modified channel was observed during the entire course of the experiment. Data were filtered at 1,200 Hz bandwidth. The solutions were 540 Na//514 Na. Temperature: 4°C. The arrowheads at the right of each trace indicate the current level of the closed state. (*B*) Voltage dependence of the probability of opening (P_o) of a BTX-modified Na^+ channel. The data points correspond to the same experiment as in Fig. 1*A*. The solid line was drawn according to the expression: $P_o = 1/\{1 + \exp[-z_1F(V - V_1)/RT](1 + \exp[-z_2F(V - V_2)/RT])\}$, and the parameters found were $V_1 = -117.47, z_1 = 0.84, V_2 = -72.87$, and $z_2 = 3.54$. The curve described by the dashed line is the fit to a single Boltzmann distribution, where: $P_o = 1/\{1 + \exp[-zF(V - V_o)/RT]\}$. The parameters obtained were: $z = 2.95$ and $V_o = -78.7$ (see also Table 1). Experiment: AG1687.

e-fold per 5.5 mV. This voltage dependence is very similar to that of the unmodified channel in the same preparation (Hodgkin and Huxley, 1952; Stimers et al., 1985). As found in other excitable cells (Huang et al., 1982), BTX shifted the voltage activation curve by ~60 mV in the hyperpolarizing direction (see also Tanguy and Yeh, 1988, 1991). Table 1 summarizes the Boltzmann parameters of the squid axon BTX-modified Na^+ channel from four different single channel experiments. The data shown in Table 1 were obtained by fitting the P_o vs. V relations to single Boltzmann distributions (Eq. 2). Since a double Boltzmann distribution would be overdetermined in cases where there are not enough data points to span all the range of potential of interest, single Boltzmann distributions were considered more fit when comparing all the data available from experiments done at different temperatures and in different axons. In the particular case of the data shown in Fig. 1 *B* (Table 1, experiment AG1687), the midpoint value for a single Boltzmann distribution (*dashed line*) was obtained at −78.7 mV.

The values for the equivalent number of gating particles, z (mean of 3.58), for the squid axon BTX-modified Na^+ channel, and for the voltage at which the channel is open 50% of the time, V_o (Table 1), obtained from a Boltzmann distribution of the form

$$P_o = [1 + \exp[-zF(V - V_o)/RT]]^{-1}, \quad (2)$$

are in reasonable agreement with the same parameters obtained for the BTX-modified Na^+ channel from squid optic nerve incorporated into planar bilayers (z = 3.7 electronic charges per channel, V_o = −89 mV; Behrens et al., 1989). The Boltzmann parameters for the squid axon BTX-modified sodium channel also agreed with those reported for BTX-modified Na^+ channels from other tissues (e.g., French et al., 1986; Recio-Pinto et al., 1987).

For a given temperature, the midpoint values were found to change depending on the particular ionic conditions used. The general trend being that the midpoint value was displaced towards more depolarized potentials whenever internal solutions with a lower ionic strength were used. This phenomenom could be a consequence of fixed charges located near the gating machinery of the channel as has been proposed for other BTX-modified sodium channels (Cukierman et al., 1988; Cukierman and Krueger, 1990; Cukierman, 1991). In low ionic strength, an internal negative fixed charge near the region of the channel involved in channel activation could be sensed by the channel as if a more hyperpolarized potential is being imposed (cf. experiments AG1687 and AG1189 of Table 1). In order to quantitate this effect, however, a more systematic study is needed because variability among axons and patches is observed (see for example Table 1, experiments JN1788 and JN2188).

TABLE 1 Basic parameters of BTX-modified Na^+ channels

Experiment	Solutions	T(°C)	z	V_o(mV)
JN1788	540 Na//530 Na	5	3.37	−85.7
		15	3.73	−79.6
JN2188	540 Na//530 Na	5	3.24	−69
		15	3.46	−65.8
AG1687	540 Na//514 Na	4	2.95	−78.7
AG1189	540 Na//50 Na	0	3.7	−67.5
		3.4	3.6	−63.9
		3.7	3.6	−66.8
		8.5	4.0	−61.2
		14.3	4.1	−57.6

Single-channel records obtained at a holding voltage of −60 mV and at different temperatures are shown in Fig. 2. Notice that an increase in temperature speeds up channel kinetics and decreases the probability of finding the channel open. Increasing the temperature also increases channel conductance and this effect has been quantified by Correa et al. (1991). For the channel conductance the enthalpic change was 6.25 kcal/mol, which corresponds to a Q_{10} = 1.53 in the 5 to 15°C range. Fig. 3 *A* shows the effect of temperature on P_o. Increasing temperature causes the P_o vs. V curve to shift to the right along the voltage axis. Changes in temperature did not significantly alter the channel voltage dependence. The voltage activation curve was displaced by 10 mV when the bath temperature increased from 0 to 14°C. The direction of the shift implies that an increase in temperature stabilizes the closed or destabilizes the open configuration of the channel, because larger depolarizing voltages are needed to obtain the same P_o. Stability of the P_o vs. V curves was checked by returning to 3.9 and 3.7°C at the middle and at the end of the runs (Fig. 3 *A*). Table 1 shows that the effective gating charge, z, was not significantly altered by temperature. Table 1 also shows that the shift of P_o to the right was observed consistently on raising the temperature.

The thermodynamic meaning of the shift of the P_o vs. voltage curve is difficult to visualize in complicated kinetic models, but if for the sake of simplicity a two-state model is considered, it leads to a simple result. Assuming that Eyring's rate theory applies to motions in proteins, the forward rate constant k_f, is given by the expression

$$k_f = (kT/h) \exp[(-\Delta H_f + T\Delta S_f + z_f FV)/RT], \quad (3)$$

where k is the Boltzmann constant, T the absolute temperature, h is the Planck constant, ΔH_f the enthalpic

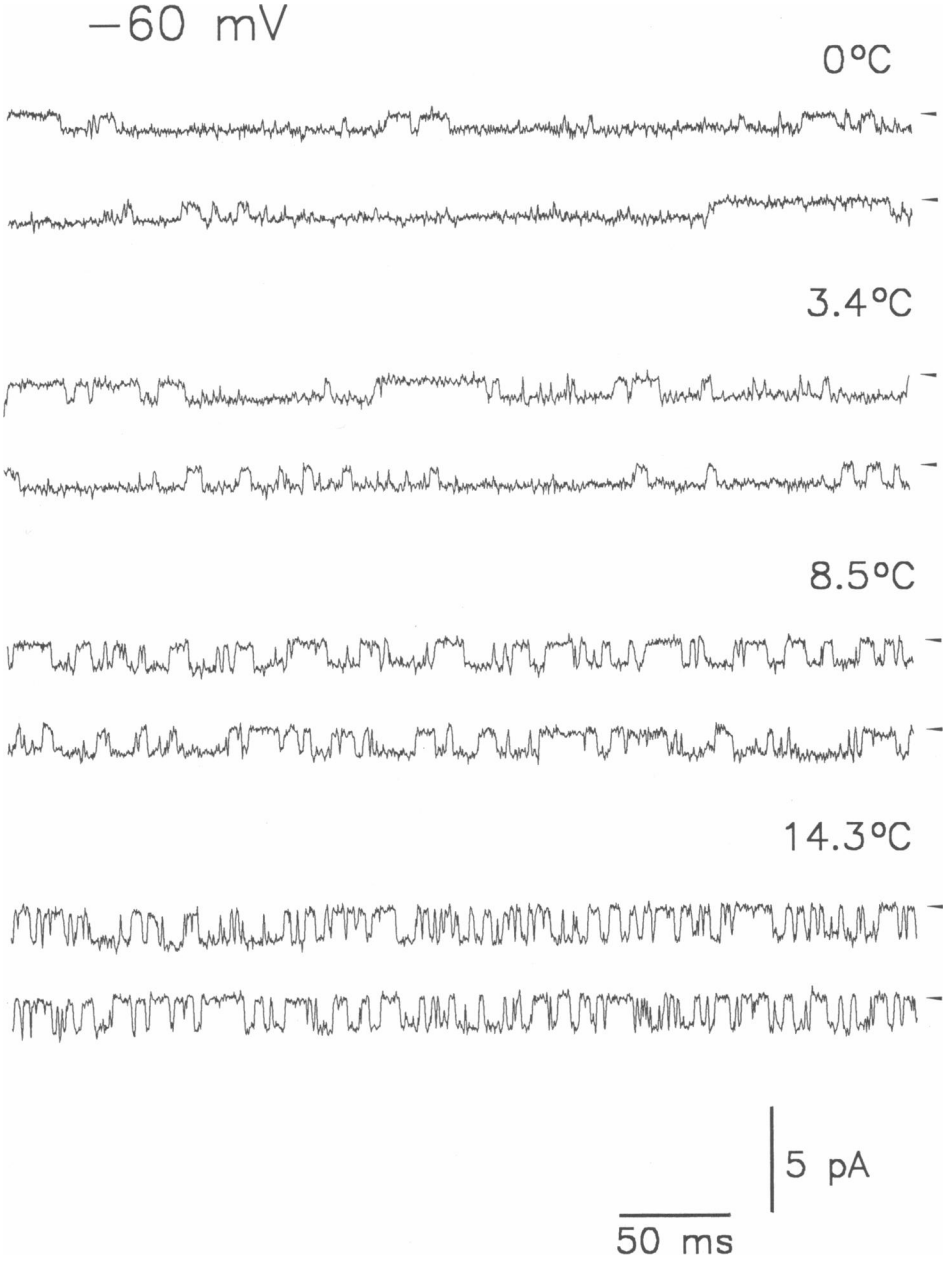

FIGURE 2 Temperature dependence of gating of a BTX-modified channel. The records shown were obtained from the same patch containing a single modified channel and were taken at the indicated temperatures. The holding potential was −60 mV. Arrowheads point to the current level of the closed state. Solutions were 540 Na//50 Na. Current records were filtered at 1,000 Hz.

change, ΔS_f the entropic change, and z the apparent number of gating particles associated with the forward reaction. Similarly, the backward rate constant can be expressed as:

$$k_b = (kT/h) \exp[(-\Delta H_b + T\Delta S_b - z_b FV)/RT], \quad (4)$$

where the terms have the same meaning as in Eq. 3 but for the backward reaction. Taking the ratio between Eqs. 4 and 3 we get

$$k_b/k_f = \exp[(\Delta H - T\Delta S - zFV)/RT], \quad (5)$$

where $\Delta H = \Delta H_f - \Delta H_b$ and $\Delta S = \Delta S_f - \Delta S_b$ are the overall changes in enthalpy and entropy associated with the closed–open reaction, with $z = z_f + z_b$ being the overall apparent gating charge involved in the same reaction (see Eq. 1). It is clear that when $V = V_o$

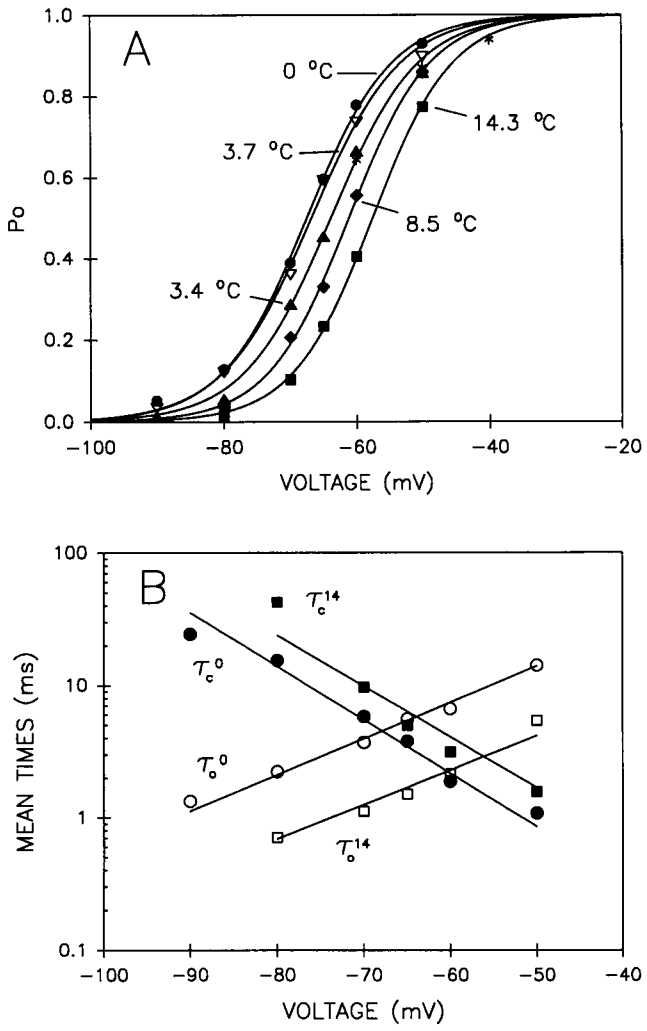

FIGURE 3 (*A*) Probability of opening (P_o) at several temperatures. The control P_o was determined from recordings made at 3.4°C at the indicated voltages (*filled triangles*). The bath temperature was then varied according to the following sequence: 8.5°C (*filled diamonds*), 14.3°C (*filled squares*), 3.9°C (*asterisks*), 0°C (*filled circles*), and 3.7°C (*open inverted triangles*). For each temperature, recordings at the different voltages were made after the bath temperature had stabilized. The fits to Boltzmann distributions gave V_o values equal to −67.5, −63.9, −66.8, −61.2, and −57.6 for 0, 3.4, 3.7, 8.5, and 14.3°C, respectively. The effective gating charge, z, was 3.7, 3.6, 3.6, 4, and 4.1 for 0, 3.4, 3.7, 8.5, and 14.3°C, respectively. Other experimental conditions as in Fig. 2. (*B*) Semi-logarithmic plot of mean open (τ_o) and mean closed (τ_c) times as a function of voltage at two different temperatures. Filled and open symbols represent mean closed and mean open times, respectively, at 0°C (*circles*) and at 14.3°C (*squares*). Same experiment as in part *A*. Solid lines correspond to linear regressions of the data. For more details, see text.

(P_o = ½, Eq. 2), $k_b/k_f = 1$, hence, from Eq. (5)

$$V_o(T) = (\Delta H - T\Delta S)/zF. \quad (6)$$

Therefore, if V_o is measured at two different temperatures, T_1 and T_2, from Eq. 6 we have that

$$V_o(T_2) - V_o(T_1) = -\Delta S(T_2 - T_1)/zF; \quad (7)$$

notice that if the probability curve is displaced to the right for a temperature increase, it implies a negative entropic change during channel opening.

In Fig. 3 *B* the mean open and closed times obtained at 0 and 14.3°C have been plotted as a function of voltage. The mean open time (τ_o) was obtained from the original records by dividing the time spent in the open state by the number of closures and the mean closed time was calculated as $\tau_c = (1 - P_o)\tau_o/P_o$. These measurements give the kinetic parameters of a two-state channel or the mean times of a multistate channel. As will be discussed below, a two-state channel is only a simplified description of the kinetics of the BTX-modified channel, but it gives a simple empirical way to describe the effects of temperature on channel kinetics. Fig. 3 *B* shows that the open times are more affected by temperature than the closed times, indicating that the closing reaction(s) become much faster upon temperature increase than the opening reaction(s). This result is consistent with the displacement of the midpoint of the P_o vs. V curve to more positive potentials as shown in Fig. 3 *A*. The voltage dependence of the open and closed times in Fig. 3 *B* were fitted to exponential functions of voltage assuming that the apparent valence is not affected by temperature (see Methods). The displacement of +11.8 mV of the intersecting fitted lines is in close agreement with the displacement of ~10 mV measured from the $P_o - V$ curves of Fig. 3 *A*.

Searching for a kinetic model: gating kinetics at 0°C

In order to obtain the most economical kinetic model able to explain the characteristics of the BTX-modified

FIGURE 4 Sample of open and closed dwell time histograms and fitted probability density functions. The continuous lines correspond to the fits (*thick lines*) and their individual components (*thin lines*). All BTX-modified single channel recordings were made at 0°C at the voltages indicated in the upper left corner of each figure. The time constants (ms) of the individual components of the fits and their relative areas (in parenthesis) were: 33.94 (0.819) and 0.47 (0.181) in *A*; 9.62 (0.025), 2.57 (0.230), and 0.30 (0.745) in *B*; 33.39 (0.017), 5.54 (0.803), and 0.52 (0.180) in *C*; 16.45 (0.407), 1.49 (0.079), and 0.41 (0.514) in *D*; 10.62 (0.050), 2.7 (0.665), and 0.3 (0.285) in *E*; 34.65 (0.472), 1.80 (0.138), and 0.37 (0.390) in *F*. The number of transitions involved were: 1318 at −50 mV (*A* and *B*), 4547 at −70 mV (*C* and *D*), and 3207 at −80 mV (*E* and *F*). Data corrected for filtering and dead time. Experimental conditions as in Fig. 2.

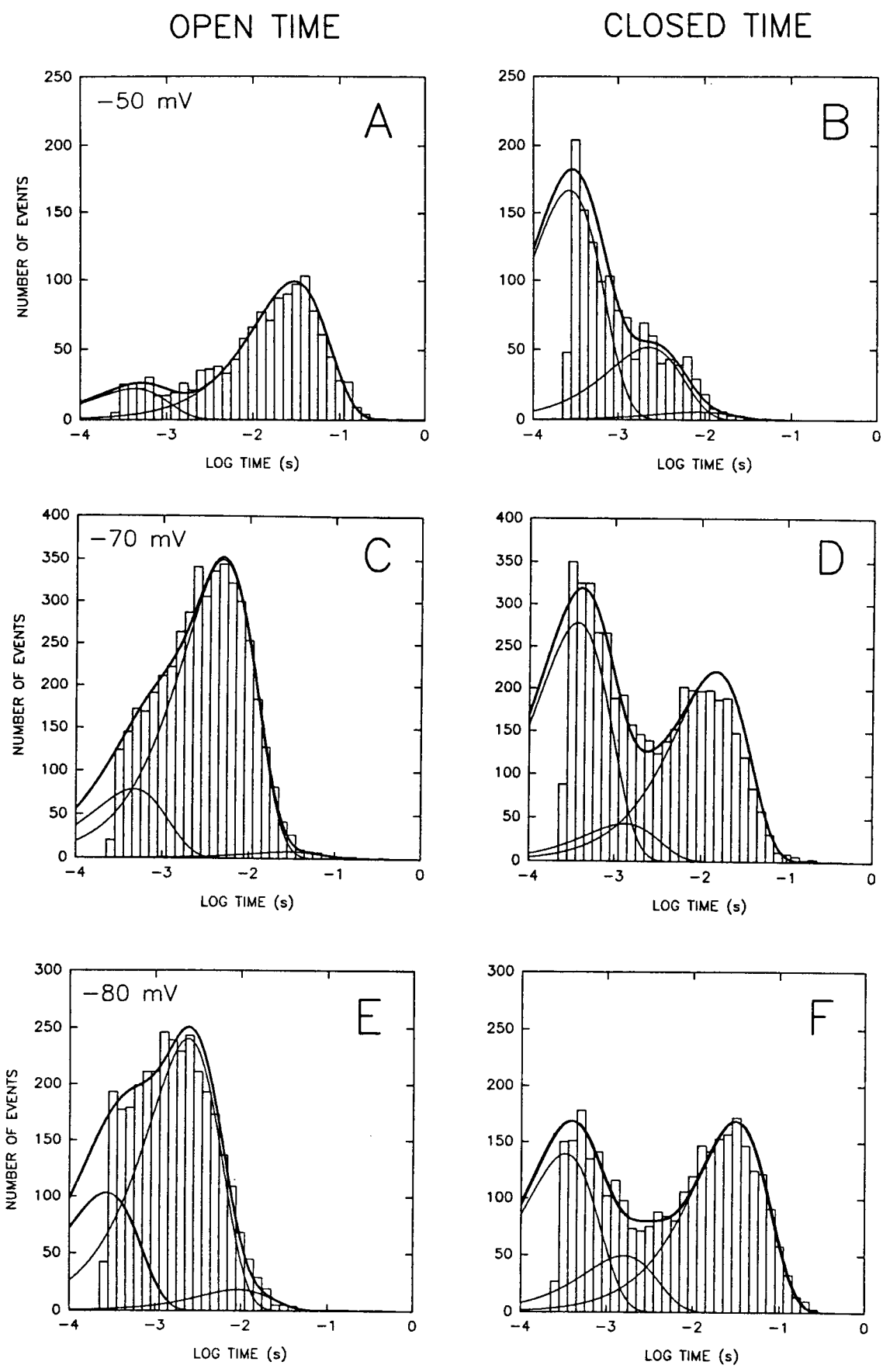
OPEN TIME
CLOSED TIME
−50 mV
A
B
−70 mV
C
D
−80 mV
E
F
NUMBER OF EVENTS
LOG TIME (s)

Na^+ channel gating we first chose to analyze in detail single-channel current records obtained at 0°C. We reasoned that since it is expected that the channel kinetics are greatly affected by temperature, experiments done at low temperatures should be more convenient to unveil the number of open and closed states of the channel.

Fig. 4 is a logarithmic histogram presentation of dwell times in the open and closed states for the BTX-modified Na^+ channel at 0°C for three different voltages. Probability density distributions of dwell times were constructed and fitted to the data to obtain the characteristic time constants for the distribution of open and closed times (Fig. 4, *thick solid lines*). At all the voltages studied, open dwell times were well described by two clearly distinguishable kinetic components (e.g., Fig. 4 *A*, *thin lines*). However, at voltages more negative than −60 mV (e.g., histograms shown in Figs. 4 and 9) a quite slow kinetic process was revealed, but accounted only for a small fraction of the total number of openings (Fig. 5 *C*). These results suggest that the squid axon BTX-modified channel has at least three open states. Voltage affects mainly the position of the peak of the major component (τ_{oi}), while the short duration component (τ_{of}) is relatively voltage insensitive (Figs. 4 and 5, *A* and *C*). Increasing voltage causes a shift in the open time distribution towards longer durations. Fig. 5 *A* shows that τ_{oi} is exponentially dependent on voltage with a slope of 10.6 mV/*e*-fold change. The slow component, τ_{os}, is also strongly voltage dependent with a slope of 9.7 mV/*e*-fold change. Voltage, on the average, has little effect on the relative fraction of events comprising the intermediate and fast components, but increases the number of events belonging to the slow component from ~1% at −65 mV to 24% at −90 (Fig. 5 *C*).

For all voltages studied, the closed dwell time histograms are well fitted by the sum of three exponentials (Fig. 4), suggesting the presence of at least three closed states. It is clear from Fig. 4 that depolarizing potentials cause a shift in the closed time distribution towards shorter durations. Voltage affects mainly the slow component (τ_{cs}), but has little effect on the intermediate component (τ_{ci}) and the component with brief mean durations (τ_{cf}, Fig. 5 *B*). Fig. 5 *B* shows that τ_{cs} is an exponential function of voltage in the voltage range studied (−90 to −50 mV) and changes *e*-fold when the potential is changed by 17.4 mV.

How are the closed and open states connected?

A great number of kinetic models can be generated for a channel containing three open and three closed states. In the present case, and in order to simplify the analysis, we decided to consider only models with two open states, because the slow open component is not observed at all potentials and it was always a minor component of the distribution of open dwell times (see Fig. 5, *A* and *C*).

Table 2 shows a number of different kinetic models that can be generated with a channel having three closed and two open states. Notice that the models can be differentiated according to the manner the different kinetic states are connected. One can select rate constants for each model that would predict a different history for the single-channel current record but that would generate the same nonconditional distributions for the dwell times (Magleby and Weiss, 1991). For this reason, a search for the possible correlation between open and closed times was attempted first (McManus et al., 1985). Fig. 6 (*filled symbols*) shows the average duration of all open events adjacent to a closed event whose duration is inside a conditioning interval plotted against the mean duration of the specified closed interval. Results are shown for three different voltages. In all the cases tested, as the specified closed intervals became longer the mean duration of the adjacent open intervals remained approximately constant. This result indicates that there is no correlation between open and closed events making it unlikely that open states originate from separate closed states.

In order to find the most appropriate kinetic model that should enable us to calculate the different rate constants as a function of voltage and temperature, we used a maximum likelihood search of parameters for given kinetic models (see Methods) of the single channel data (Horn and Lange, 1983; Horn and Vandenberg, 1984). The models that were examined with the single channel data obtained at 0°C are shown in Table 2, along with the *AIC* ranking and the log[likelihood] relative to the largest value obtained. As all this analysis was done with dead time correction, convergence for all voltages was confirmed for only two of the models tested (see Methods), therefore the *AIC* ranking may be correct only to the extent to which the likelihoods approached their maxima.

To achieve convergence in the parameter search, in

FIGURE 5 Voltage dependence of time constants (*A* and *B*) and relative fraction of events (relative area) (*C* and *D*). Experiment at 0°C. (*A* and *B*) τ_o and τ_c are the respective open and closed time constants obtained from the individual components of the fits to open and closed dwell time distributions as those shown in Fig. 4. The subscripts *s*, *i*, and *f* stand for slow, intermediate and fast, respectively. In *A* and *B*, the lines are linear fits to the data. (*C* and *D*) Plotted with the same respective symbols are the corresponding relative areas of the time components shown in parts *A* and *B*. In *C* and *D*, the data points are connected with lines for better visualization.

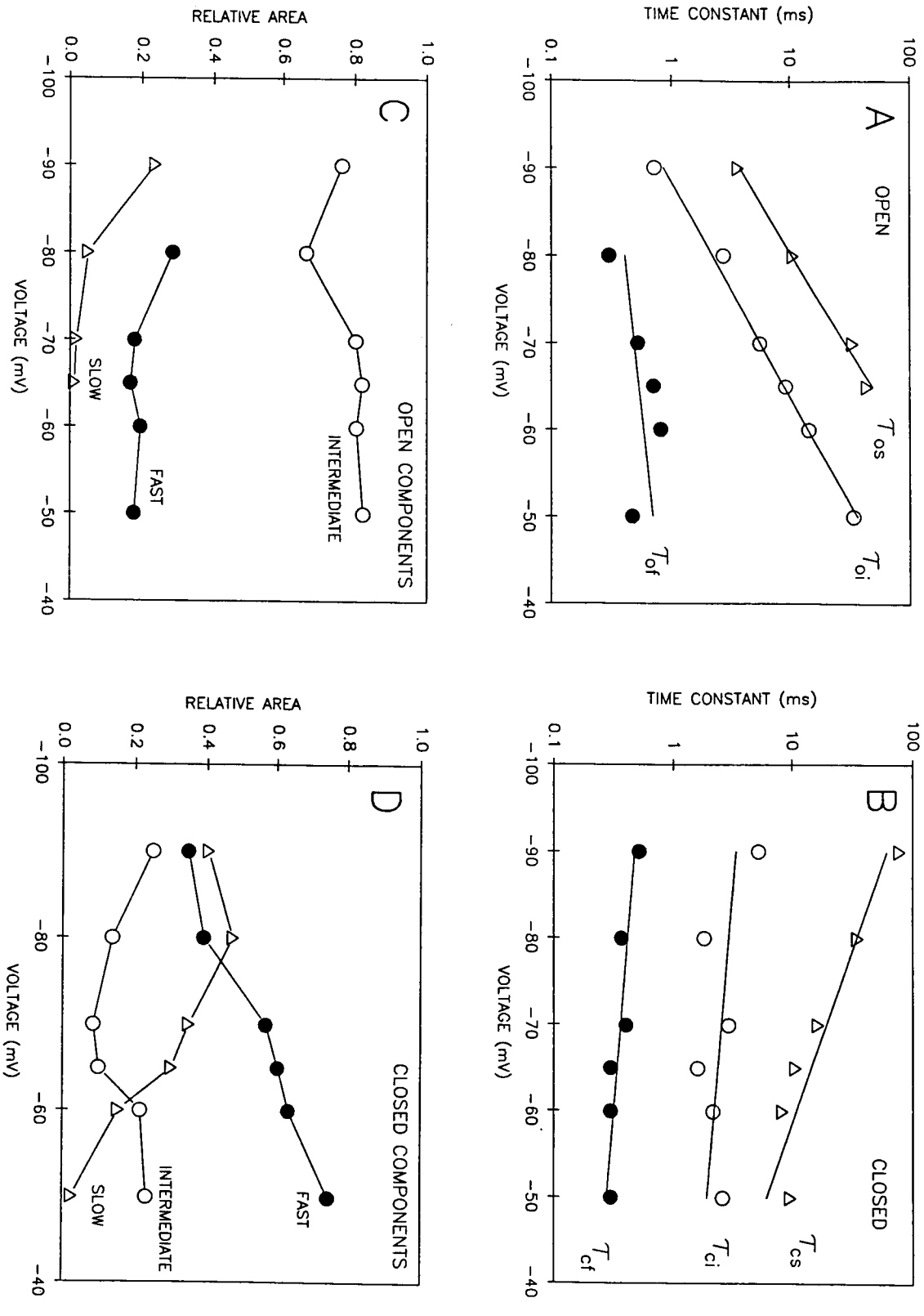
A
OPEN
TIME CONSTANT (ms)
VOLTAGE (mV)
τ_{os}
τ_{oi}
τ_{of}
B
CLOSED
τ_{cs}
τ_{ci}
τ_{cf}
C
OPEN COMPONENTS
RELATIVE AREA
INTERMEDIATE
FAST
SLOW
D
CLOSED COMPONENTS
INTERMEDIATE
FAST
SLOW

FIGURE 5

TABLE 2 **Likelihood and AIC ranking of the models tested**

	Model No. (*AIC*)	Relative log[likelihood]	Convergence
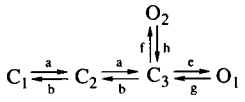	1	−11.556	+
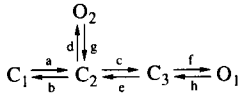	2	0	−
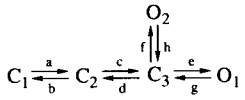	3	0.257	−
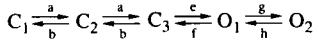	4	−12.846	+
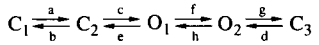	5	−242.295	−
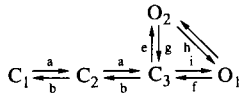	6	−382.294	−
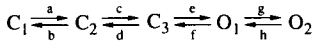	7	−497.713	−
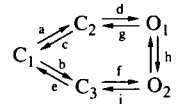	8	−548.490	−
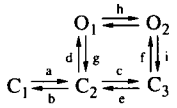	9	−657.392	−

some cases (models 3 and 7), we constrained some of the rates in the sequence to be equal (models 1 and 4). This procedure succeeded for models 1 and 4 but still failed when, in an attempt to make it more general, model 1 was circularized (model 6). Model 2 had the highest likelihood but it ranked lower in the *AIC* ranking because it contains more parameters; also, the fitting made rate *e* go to its upper bound (50,000 s^{-1}), indicating that there should be an equilibrium between the two last closed states and making model 2 similar to model 1. In addition, model 2 had a nonmonotonic voltage dependence of the rate constants. Although model 3 was better than model 1 in terms of their likelihoods (model 1 is a subhypothesis of model 3), model 1 had less parameters and predicted dwell time distributions closer to the experimental values than those predicted by model 3. Also, the rate constants fitted to model 1 had a monotonic voltage dependence as shown in Fig. 7. Other models did not converge at all or converged only partially, i.e., for some potentials only. These models ranked lower in the *AIC* ranking. Their rank level, however, has to be taken with caution. In the particular case of model 6, for instance, the expected result is a larger likelihood than that of model 1 because the latter is a particular case of the former. Since model 6 had no sure convergence, its likelihood was found to be smaller. For the same likelihood value, however, model 6 would have ranked lower than model 1 because it has one more parameter. Taking all these aspects in consideration, model 1 was chosen as the preferred model for further analysis. The rate constants obtained from it were used to generate simulated 100,000 transitions which in turn were used to generate open and closed time histograms to compare with the experimental values. Fig. 8 shows such comparison for the open and closed time distributions at three different voltages: −50, −65, and −80 mV. In the figure, the bars correspond to the experimental data at 0°C and the lines are the values predicted by model 1. In addition, the generated transitions were used to predict the conditional distribution of open intervals (*open symbols* in Fig. 6). Model 1 predicts no correlation between the duration of adjacent open and

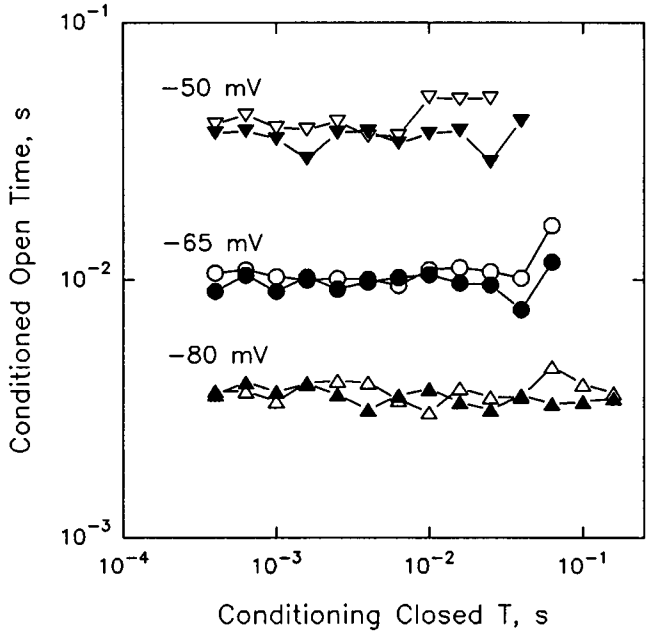

FIGURE 6 Adjacent interval analysis at three different voltages indicated at the left of the symbols. Closed symbols correspond to the experimental data at 0°C. Open symbols correspond to predicted values using model 1.

closed intervals corroborating the independent finding obtained using adjacent interval analysis of the experimental data as shown in Fig. 6 (*filled symbols*).

Effect of temperature on channel kinetics

Distributions of open and closed dwell times at several temperatures are shown in Fig. 9. At low temperature the best fit to the open and the closed durations required at least three exponential functions (see also Fig. 4). In the case of the open dwell times, at 0°C, the slowest component comprised less than 6% of the total number of transitions at all voltages studied, except −90 mV (24%) (see Fig. 5 C). Although the proportion of transitions involved in the slow component increased with temperature (see panels *A*, *C*, and *E*, Fig. 9) it was still less than 5% of the total. On the other hand, as shown in Fig. 9 *E*, the fastest component of the open time distribution is greatly reduced at high temperatures. Furthermore, the fast component of the open dwell time is lost at potentials more negative than −65 mV (data not shown). Even at voltages more positive than −65 mV, less than 7% of the events are contained in the fast component. Due to the scarcity of transitions in the slow and/or fast components of the dwell time distributions at temperatures higher than 3°C, it is difficult to quantify the effect of temperature upon these components. All that we can say at present is that the time constant of the fast component is relatively insensitive to temperature.

Fig. 10 *A* shows the voltage dependence of the time constants of the main open kinetic components (τ_{oi}) at 0, 3.4, 8.5, and 14.3°C. τ_{oi} is markedly temperature dependent. An increase in temperature from 0 to 14°C promoted a +21.2-mV parallel shift of log [τ_{oi}] towards the right along the voltage axis (dwell open times became shorter). The time constants were fitted to exponential functions of voltage assuming a valence invariant with temperature (see Methods) and the fits are shown as straight solid lines (Fig. 10 *A*). A similar analysis cannot be readily done with the closed times because there is no 'main' component; instead, the proportion of the individual components changed with voltage and temperature (see Figs. 4 and 9). A more detailed analysis on the individual transition rates fitted to model 1 at different temperatures will be presented below.

Fig. 10 *B* illustrates the effect of temperature on τ_{oi} at $V = 0$ (τ_{oi}^0) in the form of an Arrhenius plot. A linear fit to the data gave an activation energy, E_a, of 24.2 kcal/mol calculated from the slope of the line. Accordingly, the enthalpic change ($\Delta H = E_a - RT$) was found to be 23.6 kcal/mol, which is equivalent to a Q_{10} of 4.65 in the temperature range studied (0–14°C). There was no effect of potential on the temperature dependence of τ_{oi} or of τ_{os} over a range in which the time constants varied by a factor of over an order of magnitude (data not shown).

The effects of temperature on the rates of model 1

We have used the maximum likelihood estimation of the parameters of model 1 at several temperatures to determine the effect of temperature on the individual rates. Since the second open state is rarely populated at 14°C, the data at this temperature was fitted to a simplified model that contained only one open state (O_1). At 3 and 8°C both O_1 and O_2 were considered. The results of the fitting are shown in Fig. 11 *A* (*symbols*). It is apparent that rates *a*, *b*, *e*, and *g* obey a clear trend with temperature. On the other hand, rates *f* and *h* do not follow any trend with temperature which may be the result of a poor estimation of the parameters. This may be expected because these rates are in the path to the second open state which is not populated very frequently at high temperatures. Rates *a*, *b*, *e*, and *g* were fitted to exponential functions of voltage assuming that the temperature did not affect the apparent gating charge

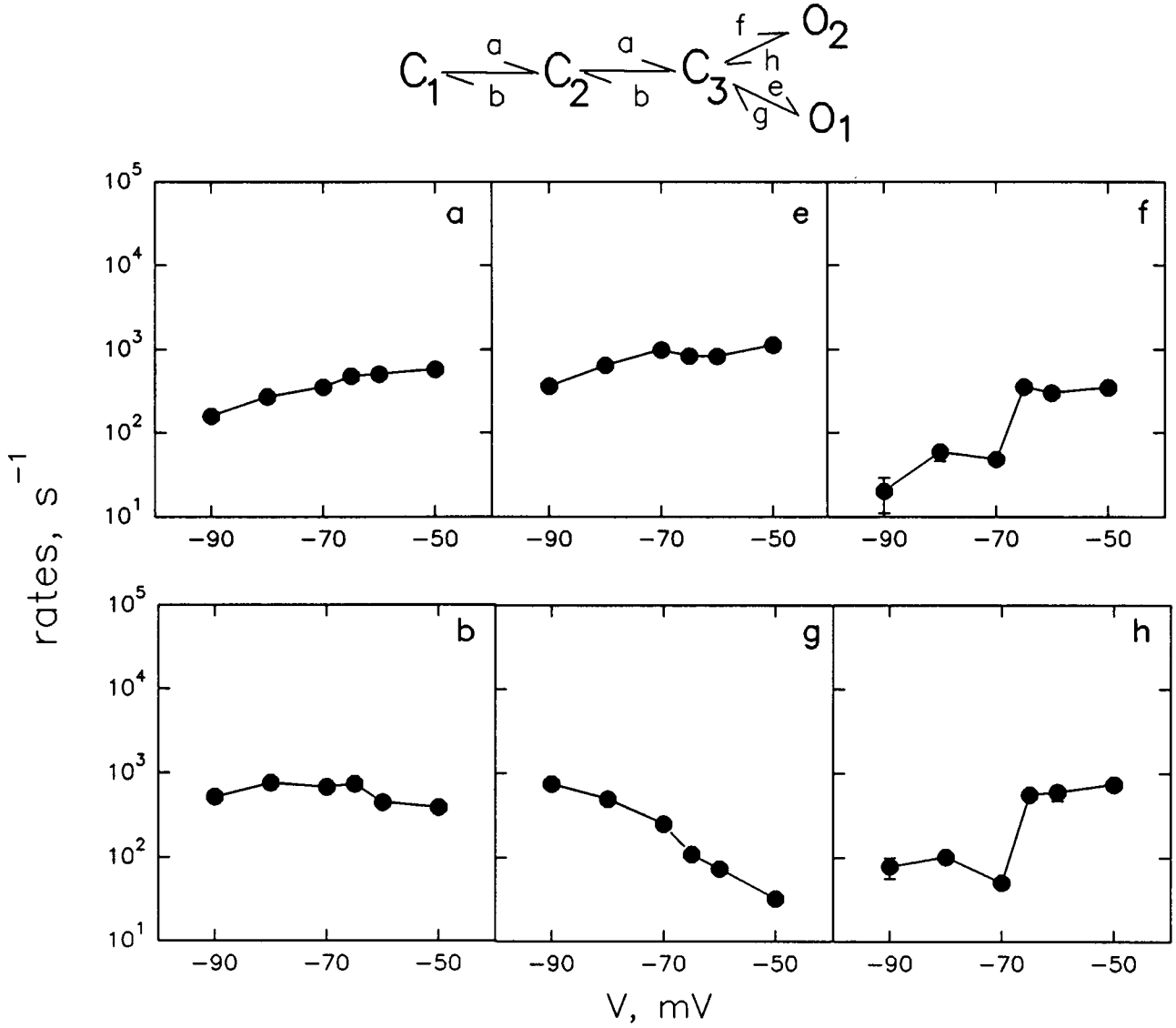

FIGURE 7 The rate constants of model 1 as a function of voltage as determined by fitting the data at 0°C for each voltage as detailed in the text. The kinetic model with its rate constants is presented in the top part of the figure.

involved in the transition (see Methods). These fits are represented by the straight lines in Fig. 11 *A*. From the slope of these fits it was possible to determine the product of the valence times the fraction of the field of each transition for both the forward and backward rates (see Eqs. 3 and 4). Also from Eqs. 3 and 4, the intercept when $V = 0$ allows the estimation of $\Delta H_x - T\Delta S_x$ for each rate at each temperature (where the subindex x is either f for forward or b for backward) which is equal to the ΔG_x. For any individual rate, the ΔH_x and the ΔS_x (assumed independent of temperature) were estimated by fitting the equation $\Delta G_x = \Delta H_x - T\Delta S_x$ to the values of ΔG_x obtained at each temperature and to their respective temperatures. The estimated parameters are shown in Table 3 and the resulting profile of the energy diagram connecting the kinetic states of the channel is shown in Fig. 11 *B*.

FIGURE 8 Example of dwell time predictions by model 1. The bars correspond to the experimental data at −50 mV (*A* and *B*), −65 mV (*C* and *D*), and −80 mV (*E* and *F*). Temperature: 0°C. The lines are the predicted values obtained from the analysis of 100,000 transitions generated with model 1 using the parameters shown in Fig. 7. Left panels are open times and right panels are closed times. For details, see text.

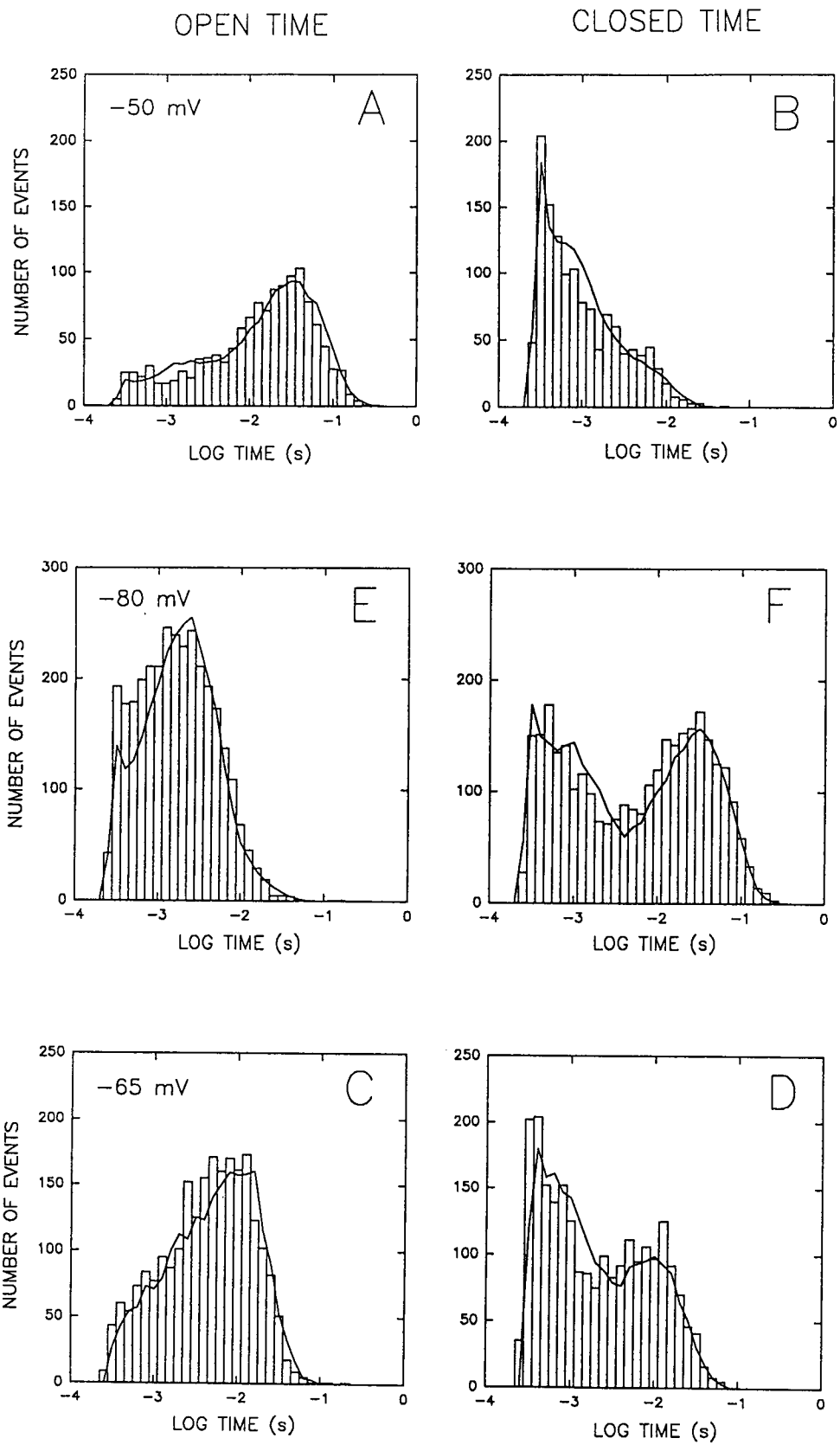
OPEN TIME
CLOSED TIME
−50 mV
A
B
−80 mV
E
F
−65 mV
C
D
NUMBER OF EVENTS
LOG TIME (s)

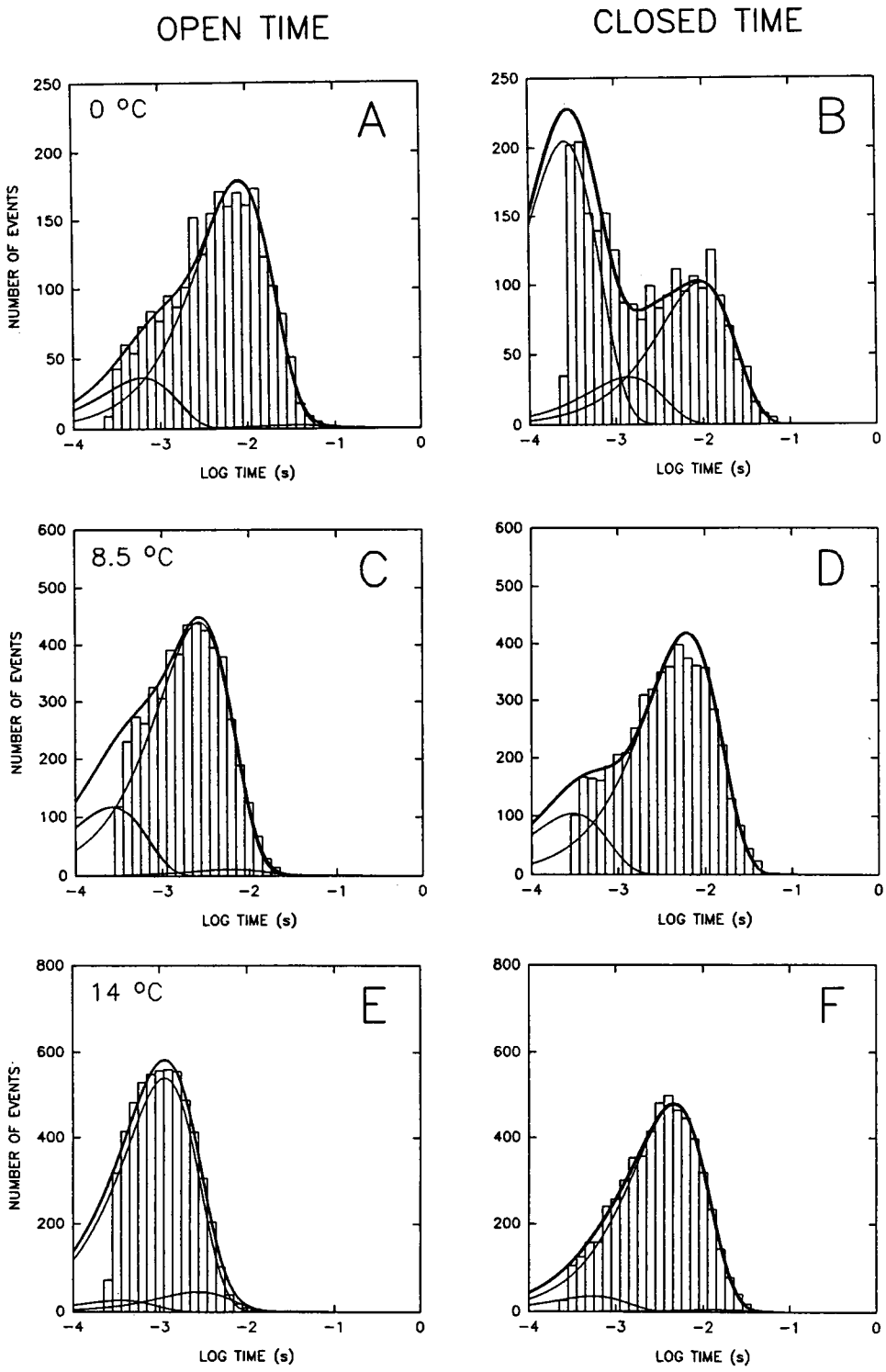

FIGURE 9 Open and closed dwell time histograms at different temperatures. The applied voltage was −65 mV. The recordings were made at the indicated temperatures (*upper left corner*). The time constants and relative areas were: 44.20 (0.011), 9.23 (0.820), and 0.71 (0.169) in *A*; 10.64 (0.299), 1.58 (0.100), and 0.30 (0.601) in *B*; 7.23 (0.019), 3.00 (0.775), and 0.30 (0.206) in *C*; 6.89 (0.801) and 0.34 (0.199) in *D*; 3.18 (0.073), 1.29 (0.885), and 0.40 (0.042) in *E*; and 15.59 (0.011), 5.16 (0.922), and 0.63 (0.067) in *F*. For further description see text and Fig. 4.

DISCUSSION

Kinetic models for the BTX-modified Na^+ channel: a comparison with previous studies

Our kinetic analysis of the BTX-modified squid axon Na^+ channel strongly suggests the presence of several closed states and more than one open state. This result differs from kinetic schemes proposed previously for the BTX-modified Na^+ channels in neuroblastoma cells (Huang et al., 1984) and in channels from several sources studied in planar lipid bilayers (French et al., 1986b; Behrens et al., 1989; Keller et al., 1986, 1990). In all previous studies, although several closed states were found, only a single open state could be detected. We think that the possibility that the squid giant axon Na^+ channel is unique in this regard is unlikely because the work of Behrens et al. (1989) was done using a membrane preparation from squid optic nerve Na^+ channels incorporated into lipid bilayers. We argue here that the reason for not detecting a second open state in previous studies resides mainly in the difference in temperature at which previous kinetic measurements were done in a temperature range (usually ~20°C) in which the fast open time constant would be too fast to be detected. Our results show that above 8°C it becomes difficult to detect the fast openings. In the squid Na^+ channel we have also detected a slow kinetic component in the distribution of the open lifetimes. It is possible that this state was not found before because most previous studies used linear representation of the dwell time distributions. As pointed out by Sigworth and Sine (1987), kinetic components, which are a small fraction of the total number of events and well separated from the rest, are hardly visible in this kind of representation unless the appropriate time scales are used and several thousands of transitions are considered for the overall analysis.

In brain Na^+ channels incorporated into planar lipid bilayers there is no correlation between adjacent channel open and closed dwell times (Keller et al., 1986, 1990). In agreement with those results, we found that the duration of adjacent open and closed intervals are uncorrelated. Jackson et al. (1983) were the first to point out that kinetic models in which there is only one closed state capable of leading to an opening (models 1, 3, 4, 6, and 7 in Table 2) give rise to uncorrelated open-state durations. On the other hand, in models 2, 5, 8, and 9 one would find correlation between adjacent intervals only if the interconversion between closed states (mod-

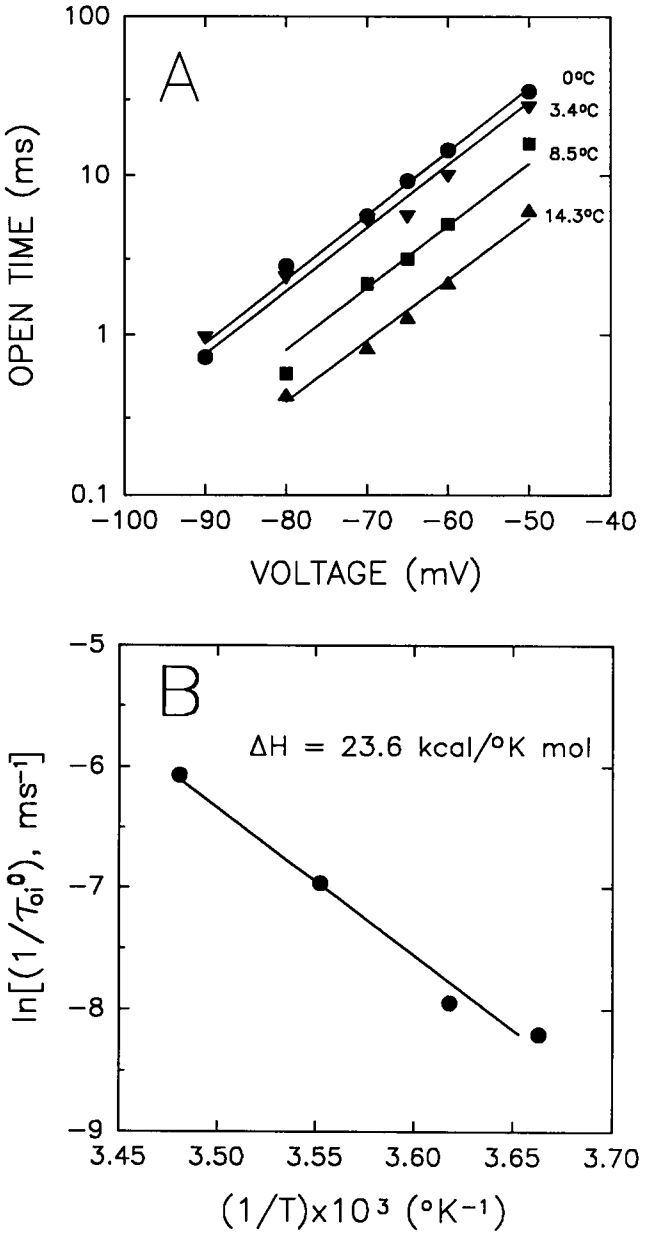

FIGURE 10 (*A*) The voltage dependence and temperature dependence of the main component of the open times. The straight lines correspond to the fitted rates assuming that the apparent valence does not change with temperature. From the fit, the values of the valence and the chemical free energy change (ΔG) were obtained for each temperature. (*B*) Arrehnius plot of the chemical part of the energy barrier of the open to close transition of the main open component. τ_{oi}^0 is the time constant of the main open component at 0 mV. This curve was generated with the ΔG values extracted from the fits of part *A* of this figure.

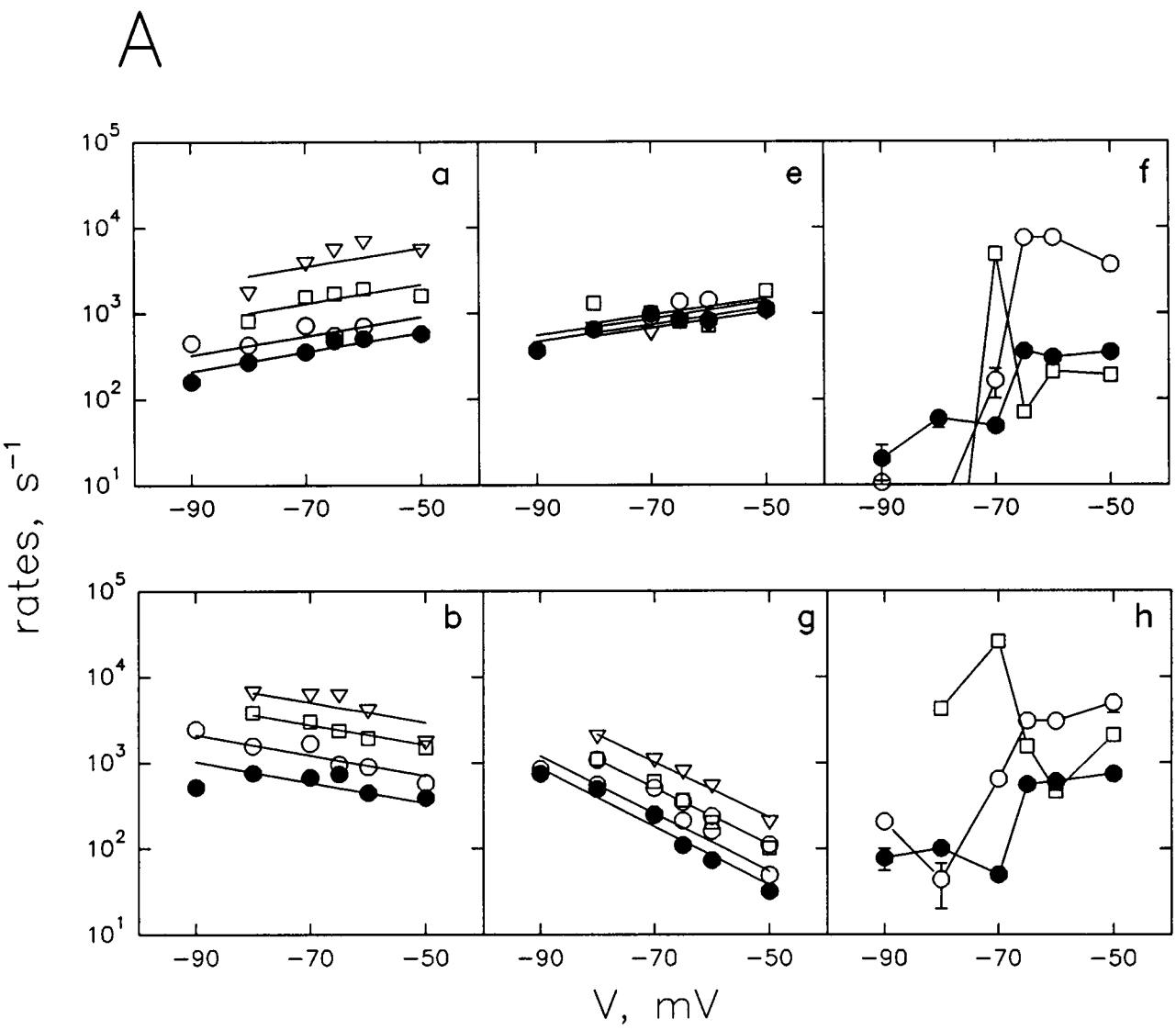

FIGURE 11

els 2 and 9) or open states (models 5 and 8) were slow. If the equilibrium between these states is fast, little or no correlation is expected to be found.

The preferred model, model 1, consists of three closed states and two open states connected to the same closed state. This model is not expected to generate correlation in the open–close times and it does reproduce the conditional dwell times and the open and closed times rather well. Single channel recordings are mostly useful to estimate rates very close to the open states because those are the experimentally observed events. The rates between closed states that are far from the open state are poorly estimated and make the convergence of the algorithm more difficult. In the model presented here, the transition rates between the closed states were constrained to be equal to effectively decrease the number of parameters to be estimated, thus improving the convergence of the numerical curve fitting procedure. When the rates between closed states are left unconstrained the likelihood decreases and convergence to a minimum is not confirmed. Therefore, the fact that the rates connecting the closed states are equal should only be considered as tentative. To pinpoint the actual correlation between the rates of the closed states other types of experiments are required, such as gating currents measurements.

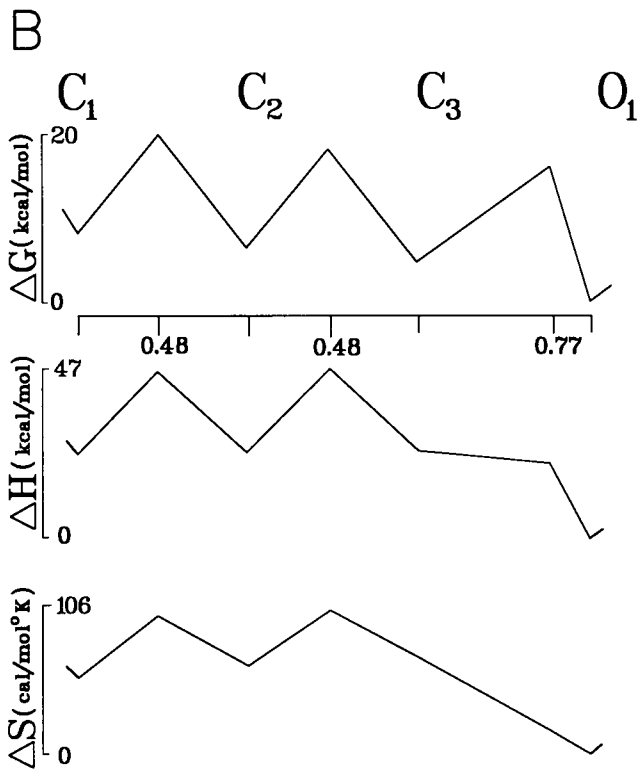

FIGURE 11 (*A*) The voltage and temperature dependence of the rates predicted by model 1. The letters at the top right corner of each graph are the represented rate constants (for reference to the model see Fig. 7). Each symbol represents a different temperature: filled circles, 0°C; open circles, 3.4°C; squares, 8.5°C; and inverted triangles, 14.3°C. The straight lines are the fitted voltage dependence of rates *a*, *b*, *e*, and *g* assuming a valence independent of the temperature. Rates *f* and *h* were not fitted. (*B*) The energy profile of model 1. The fits shown in part *A* of this figure gave a value of the effective charge for each transition (forward or backward). In the diagram, the fraction of the field where the peak of the barrier is located is indicated for each of the three barriers (0.48, 0.48, and 0.77). The fraction of the field times the total valence is the effective charge which is also shown Table 3. In addition, the fits shown in part *A* of the figure gave four values (one per temperature) of ΔG for each transition. These ΔG values were fitted to $\Delta H - T\Delta S$ to obtain the entropy and enthalpy changes represented in the diagram.

Channel kinetics and Eyring energy barriers

The main effect of an increase in temperature on channel kinetics can be summarized as an increase in transition rates and a shift of the open probability to more positive potentials. The simplified steady-state analysis shows that there is a decrease in entropy during the opening of the BTX-modified channel. Most of the shift of the P_o is the result of an increase in the closing rates with less effect of temperature on the opening rates. An increase in temperature seems to favor the closed states over the open configuration, and this agrees with the notion that the open states are more ordered than the closed states.

TABLE 3 **Parameters of the energy barriers of the rates in model 1**

Rate	z	ΔH_x^*	ΔS_x^*	$T\Delta S_x^*(T = 0°C)$	Q_{10}
		kcal/mol	*cal/°Kmol*	*kcal/mol*	
a	0.61	23.5 ± 1	47.7 ± 3.8	13.0 ± 1	5.05
b	−0.66	23.3 ± 0.2	35.9 ± 8.7	9.8 ± 2.4	4.55
e	0.05	−2.5 ± 2.7	−52.2 ± 9.6	−14.3 ± 2.6	−0.98
g	−1.83	21.2 ± 0.6	18.9 ± 2	5.2 ± 0.5	3.99

*x can be either f for the forward rates *a* and *e*, or *b* in the backward direction for rates *b* and *g*.

The fitting of the temperature data to model 1 gave more insight on the energy barriers involved in the changes of channel configuration (see Fig. 11 *B*). The transitions between closed states involve about half of the total gating charge (see Table 3). The other half is moved in the transition between the last closed state and the principal open state, but most of the voltage dependence occurs in the return from the open to the closed state. The energy changes involved in the transitions between closed states are mainly enthalpic with some entropy contribution in evolving from state C_1 to C_3 (see Table 3). The activation energy of the transition between C_3 and O_1 is purely entropic with a small negative enthalpic change (which could be zero because the standard error of the fitted value is as large as the value). On the other hand, the activation energy of the reverse reaction has a large enthalpic and positive entropic components. These values suggest that the evolution of the channel from the most closed state to the open state involves first a series of normal chemical reactions which could be the breaking and making of salt bridges and/or hydrogen bonds. In the last stage, when the channel has to overcome the energy barrier between the last closed state and the open state, the main process seems to be a reorganization of the molecule that decreases the degrees of freedom of the involved channel components rendering the system more ordered.

Mode of action of batrachotoxin

During a maintained membrane depolarization unmodified Na^+ channels inactivate. Bezanilla and Armstrong (1974) found that if the inactivation process is let to proceed normally, the gating charge recovered in the "off" of the voltage step is less than the gating charge mobilized during the "on" of the pulse. In this case the charge is said to be immobilized. In the ball-and-chain

model (Armstrong and Bezanilla, 1977), the ball (inactivation particle) interacts with a receptor contained in the inner mouth of the channel hindering the passage of Na^+ completely. In this model charge immobilization is presumably a consequence of electrostatic interactions between the inactivation particle bound to the channel mouth and the activation particles making more difficult the return of the latter to their original state. Charge immobilization has been observed in many other voltage-dependent Na^+ channels (Rudy, 1976; Nonner, 1980; Starkus et al., 1981; Campbell, 1983; Conti and Stuhmer, 1989).

Fast inactivation and charge immobilization are removed by agents such as pronase (Armstrong et al., 1973) and chloramine-T (Tanguy and Yeh, 1988). These results have been usually interpreted as a complete removal of the inactivation particle. On the other hand, BTX eliminates fast inactivation, but leaves charge immobilization intact (Tanguy and Yeh, 1988). This is an important observation because it suggests that BTX might be interacting with the receptor for the inactivation particle still causing charge immobilization but without blocking or perhaps partially occluding the channel.[1]

There is at present good evidence that unmodified Na^+ channels contain only one open state in the negative potential region (Horn and Vandenberg, 1984; Patlak and Ortiz, 1986; Scanley et al., 1990; Vandenberg and Bezanilla, 1991; but see Nagy, 1987). Moreover, an important piece of information that comes from single-channel recordings is that Na^+ channels can inactivate before opening (Aldrich et al., 1983; Horn and Vandenberg, 1984; Scanley et al., 1990). Summing to the information from single channel studies, the information provided by gating and macroscopic current measurements, the most parsimonious kinetic model for the unmodified Na^+ channel which emerges (Vandenberg and Bezanilla, 1991), requires a pathway between closed-inactivated states in parallel with the pathway between closed states. Taking this kinetic model for the unmodified Na^+ channel at face value implies that BTX should transform the inactivated states into conducting (open) states so as to keep the process of charge immobilization intact. Of course, this does not exclude additional modification of the open state by the toxin. Kinetic models for the BTX-modified Na^+ channel that consider a single open state are not consistent with the notion of the open-inactivated state becoming conductive after-treatment with BTX. Model 1 would not predict charge immobilization by way of states in parallel with the main sequence of closed states, but it would have apparent charge immobilization if the return of charge from any of the open states (deactivation) is slow. Parallel closed states are expected because they would be equivalent to the closed-inactivated states of the normal channel; they could however stay nonconducting after BTX modification. Vandenberg and Bezanilla (1991) found that single channel data from unmodified Na^+ channels could be well predicted with only one inactivated state whereas gating current data required several inactivated states. The discrepancy is most likely due to the insensitivity of single channel records to the number and connections between closed states. We conclude that, although the complete model would have at least two inactivated states, single channel data seem unable to detect them.

Model 1 is not incompatible with the hypothesis posed by Tanguy and Yeh (1988) that the inactivated state becomes a conducting state. To keep consistency with the model for the normal channel, we may identify state O_1 in our model for the BTX-modified Na^+ channel with the open state in the unmodified channel and state O_2 with the open-inactivated state. The connection between O_1 and O_2 would become negligible in the presence of BTX. This identification, however, is not satisfactory because the dwell times of the open states do not coincide with the dwell times of the normal channel, indicating that BTX is modifying drastically all the rate constants involved in channel opening. We suggest that the increase in the duration of open events after BTX treatment resides in the appearance of the open state O_2, which may have been the inactivated state that would now be conducting and stabilized by the presence of the drug.

Finally, our results reveal the existence of at least three open states. However, in models with more than two open states the convergence of the parameters to well determined values was seldom reached. For this reason the analysis was based on only two open states. It may well be, however, that a third open state could emerge from a close-inactivated state as discussed above. But it is also possible that BTX reveals an open state that would be regularly in connection with the open state of the unmodified channel, but that is rarely populated in the voltage range of study (negative potentials). There is evidence in this same preparation for the existence of a second open state which, under normal circumstances, would only be apparent at very positive potentials or under inverse gradient conditions also at positive potentials (Bezanilla and Correa, 1991). The possibility exists that BTX would change the voltage dependence of activation of this second open state very much like the change already obvious in the P_o, making it detectable at more negative potentials.

[1]A partial occlusion of the Na^+ channel by BTX would naturally explain the reduction in channel conductance induced by the toxin reported by Quandt and Narahashi (1982) and by Correa et al. (1991).

We thank Dr. John Daly for the gift of batrachotoxin. We also thank Dr. O. Alvarez and Dr. David Naranjo for sharing their computer programs for fitting dwell times and performing the adjacent interval analysis with us.

This work was supported by the National Institutes of Health grants GM-35981 and GM-30376, the Fondo Nacional de Investigacion grant 451-1988 and 863-1991, and a grant from the Tinker Foundation. Ramóne Latorre is the recipient of a John D. Guggenheim fellowship and he wishes to thank the Dreyfus Bank for generous support from a private foundation that they made available to him.

Received for publication 29 August 1991 and in final form 19 November 1991.

REFERENCES

Akaike, H. 1974. A new look at statistical model identification. *IEEE Trans. Automatic Control.* AC-19:716–723.

Aldrich, R. W., D. P. Corey, and C. F. Stevens. 1983. A reinterpretation of mammalian sodium channel gating based on single channel recording. *Nature (Lond.).* 306:436–441.

Albuquerque, E. X., J. W. Daly, and B. Witkop. 1971. Batrachotoxin chemistry and pharmacology. *Science (Wash. DC).* 172:995–1002.

Albuquerque, E. X., I. Seyama, and T. Narahashi. 1973. Characterization of batrachotoxin-induced depolarization of the squid giant axon. *J. Pharmacol. Exp. Ther.* 184:308–314.

Armstrong, C. M., and F. Bezanilla. 1977. Inactivation of the sodium channel. II Gating current experiments. *J. Gen. Physiol.* 70:567–590.

Armstrong, C. M., F. Bezanilla, and E. Rojas. 1973. Destruction of sodium conductance inactivation in squid axons perfused with pronase. *J. Gen. Physiol.* 62:375–391.

Behrens, M. I., A. Oberhauser, F. Bezanilla, and R. Latorre. 1989. Batrachotoxin-modified sodium channels from squid optic nerve in planar bilayers. Ion conduction and gating properties. *J. Gen. Physiol.* 93:23–41.

Bezanilla, F. 1985. A high capacity data recording device based on a digital audio processor and a video cassette recorder. *Biophys. J.* 47:437–441.

Bezanilla, F. 1987. Single sodium channels from the squid giant axon. *Biophys. J.* 52:1087–1090.

Bezanilla, F., and C. M. Armstrong. 1974. Gating currents of the sodium channels: three ways to block them. *Science (Wash. DC). 183:753–754.*

Bezanilla, F., and A. M. Correa. 1991. Single sodium channels in high internal sodium in the squid giant axon. *Biophys. J.* 59:12*a*. (Abstr.)

Bezanilla, F., and C. Vandenberg. 1990. The cut-open axon technique. *In* Squid as Experimental Animals. D. L. Gilbert, W. J. Adelman, Jr., and J. M. Arnold, editors. Plenum Press, New York. 153–159.

Blatz, A. L., and K. L. Magleby. 1989. Adjacent intervals analysis distinguishes among gating mechanisms for the fast chloride channel from rat skeletal muscle. *J. Physiol. (Lond.).* 410:561–585.

Campbell, D. T. 1983. Sodium channel gating currents in frog skeletal muscle. *J. Gen. Physiol.* 82:679–701.

Conti, F., and W. Stuhmer. 1989. Quantal charge redistributions accompanying the structural transitions of sodium channels. *Eur. Biophys. J.* 17:53–59.

Correa, A. M., and F. Bezanilla. 1988. Properties of BTX-treated single Na channels in squid axon. *Biophys. J.* 53:226*a*. (Abstr.)

Correa, A. M., R. Latorre, and F. Bezanilla. 1989. Na-dependence and temperature effects on BTX-treated sodium channels in the squid axon. *Biophys. J.* 55:403*a*. (Abstr.)

Correa, A. M., R. Latorre, and F. Bezanilla. 1991. Ion permeation in normal and batrachotoxin-modified Na^+ channels in the squid giant axon. *J. Gen. Physiol.* 97:605–625.

Colquhoun, D., and F. J. Sigworth. 1983. Fitting and statistical analysis of single-channel records. *In* Single-Channel Recording. B. Sakmann and E. Neher, editors. Plenum Press, New York. 191–263.

Cukierman, S. 1991. Asymmetric electrostatic effects on the gating of rat brain sodium channels in planar lipid membranes. *Biophys. J.* 60:845–855.

Cukierman, S., and B. K. Krueger. 1990. Modulation of sodium channel gating by external divalent cations studied in planar lipid bilayers. Differential effects on opening and closing rates. *Pfluegers Arch.* 416:360–369.

Cukierman S., W. C. Zinkand, R. J. French, and B. Krueger. 1988. Effects of membrane surface charge and calcium on the gating of rat brain sodium channels in planar bilayers. *J. Gen. Physiol.* 92:431–477.

Daly, J. W., C. W. Myers, and N. Whittaker. 1987. Further classification of skin alkaloids from neotropical poison frogs (*Dendrobatidae*), with a general survey of toxin/noxious substances in the amphibian. *Toxicon.* 25:1023–1095.

Daly, J. W., and B. Witkop. 1971. Batrachotoxin, an extremely active cardio- and neurotoxin from the Colombian arrow posion frog *Phyllobates aurotaenia. Clin. Toxicol.* 4:331–342.

Daly, J. W., B. Witkop, P. Bommer, and K. Biemann. 1965. Batrachotoxin, the active principle of the Colombian arrow poison frog, *Phyllobates bicolor. J. Am. Chem. Soc.* 87:124–126.

French, R. J., B. K. Krueger, and J. F. Worley. 1986a. From brain to bilayer. Sodium channels from rat neurons incorporated into planar lipid membranes. *In* Ionic Channels in Cells and Model Systems. R. Latorre, editor. Plenum Press, New York. 273–290.

French, R. J., J. F. Worley, M. B. Blaustein, W. O. Romine, K. K. Tam, and B. Krueger. 1986b. Gating of batrachotoxin-activated sodium channel in lipid bilayers. *In* Ion Channel Reconstitution. C. Miller, editor. Plenum Press, New York. 363–383.

Garber, S. 1988. Symmetry and asymmetry of permeation through toxin-modified Na^+ channels. *Biophys. J.* 54:767–776.

Green, W. N., L. B. Weiss, and O. S. Andersen. 1987. Batrachotoxin-modified sodium channels in lipid bilayers. Ion permeation and block. *J. Gen. Physiol.* 89:841–872.

Hamill, O. P., A. Marty, E. Neher, B. Sackmann, and F. Sigworth. 1981. Improved patch clamp techniques for high resolution current recording from cells and from cell-free membrane patches. *Pfluegers Arch.* 381:85–100.

Hille, B. 1984. Ionic Channels of Excitable Membranes. Sinahuer Associates, Inc., Sunderland, MA. 249–271.

Hodgkin, A. L., and A. F. Huxley. 1952. A quantitative description of the membrane current and its application to conduction and excitation in nerve. *J. Physiol. (Lond.)* 117:500–544.

Horn, R., and K. Lange. 1983. Estimating kinetic constant from single-channel data. *Biophys. J.* 43:207–223.

Horn, R., and C. Vandenberg. 1984. Statistical properties of single sodium channels. *J. Gen. Physiol.* 84:505–534.

Huang, L.-Y. M., A. Catterall, and G. Ehrenstein. 1979. Comparison of ionic selectivity of batrachotoxin-activated channels with different tetrodotoxin dissociation constants. *J. Gen. Physiol.* 73:839–854.

Huang, L.-Y. M., N. Moran, and G. Eherenstein. 1982. Batrachotoxin modifies the gating kinetics of sodium channels in internally perfused neuroblastoma cells. *Proc. Natl. Acad. Sci. USA.* 79:2082–2085.

Huang, L.-Y. M., N. Moran, and G. Ehrenstein. 1984. Gating of batrachotoxin-modified sodium channels in neuroblastoma cells determined from single-channel measurements. *Biophys. J.* 45:313–322.

Huang, L.-Y., A. Yatani, and A. M. Brown. 1987. The properties of batrachotoxin-modified cardiac Na channels, including state dependent block by tetrodotoxin. *J. Gen. Physiol.* 90:341–360.

Jackson, M. B., B. Wong, C. E. Morris, H. Lecar, and C. N. Christian. 1983. Successive openings of the same acetylcholine receptor channel are correlated in time. *Biophys. J.* 42:109–114.

Keller, B. U., R. P. Hartshorne, J. A. Talvenheimo, W. A. Catterall, and M. Montal. 1986. Sodium channels in planar lipid bilayers. Channel kinetics of purified sodium channels modified by batrachotoxin. *J. Gen. Physiol.* 88:1–23.

Keller, B. U., M. S. Montal, R. P. Hartshorne, and M. Montal. 1990. Two-dimensional probability density analysis of single channel currents from reconstituted acetylcholine receptors and sodium channels. *Arch. Biochem. Biophys.* 276:47–54.

Khodorov, B. I. 1985. Batrachotoxin as a tool to study voltage sensitive sodium channels of excitable membranes. *Prog. Biophys. Mol. Biol.* 45:57–148.

Khodorov, B. I., and S. V. Revenko. 1979. Further analysis of the mechanisms of action of batrachotoxin on the membrane of myelinated nerve. *Neuroscience.* 4:1315–1330.

Llano, I., C. K. Webb, and F. Bezanilla. 1988. Potassium conductance of the squid giant axon. Single channel studies. *J. Gen. Physiol.* 92:179–196.

Magleby, K. L., and D. S. Weiss. 1991. Estimating kinetic parameters for single channels with simulation. A general method that resolves the missed event problem and accounts for noise. *Biophys. J.* 58:1411–1426.

McManus, O. B., A. L. Blatz, and K. L. Magleby. 1985. Inverse relationship of the durations of adjacent open and shut intervals for Cl and K channels. *Nature (Lond.).* 317:625–627.

Moczydlowski, E., S. Garber, and C. Miller. 1984. Batrachotoxin-activated sodium channels in planar lipid bilayers: competition of tetrodotoxin block by Na. *J. Gen. Physiol.* 84:665–686.

Nagy, K. 1987. Evidence for multiple open states of sodium channels in neuroblastoma cells. *J. Membr. Biol.* 96:251–262.

Nonner, W. 1980. Relations between the inactivation of sodium channels and the immobilization of gating charge in frog myelinated nerve. *J. Physiol. (Lond.).* 299:573–603.

Patlak, J., and M. Ortiz. 1986. Two modes of gating during late Na^+ channel currents in frog sartorius muscle. *J. Gen. Physiol.* 87:305–326.

Quandt, F. N., and T. Narahashi. 1982. Modification of single Na^+ channels by batrachotoxin. *Proc. Natl. Acad. Sci. USA.* 79:6732–6736.

Recio-Pinto, E., D. S. Duch, S. R. Levinson, and R. W. Urban. 1987. Purified and unpurified sodium channels from the eel electroplax in planar lipid bilayers. *J. Gen. Physiol.* 90:375–395.

Rojas, E., and B. Rudy. 1976. Destruction of the sodium conductance inactivation by a specific protease in perfused fibers of *Loligo*. *J. Physiol. (Lond.).* 262:477–494.

Roux, B., and R. Sauve. 1985. A general solution to the time interval omission proble applied to single channel analysis. *Biophys. J.* 48:149–158.

Rudy, B. 1976. Sodium gating currents in Myxicola giant axons. *Proc. Roy. Soc. Lond. B.* 193:469–475.

Scanley, B. E., D. A. Hanck, T. Chay, and H. A. Fozzard. 1990. Kinetic analysis of single sodium channels from canine cardiac purkinje cells. *J. Gen. Physiol.* 95:411–4377.

Sigworth, F., and S. M. Sine. 1987. Data transformation for improved display and fitting of single-channel dwell time histograms. *Biophys. J.* 52:1047–1054.

Starkus, J. G., B. D. Fellmeth, and M. D. Rayner. 1981. Gating currents in the intact crayfish giant axon. *Biophys. J.* 35:521–533.

Stimers, J. R., F. Bezanilla, and R. E. Taylor. 1985. Sodium channel activation in the squid giant axon. Steady-state properties. *J. Gen. Physiol.* 85:65–82.

Tanguy, J., and J. Z. Yeh. 1988. Batrachotoxin uncouples charge immobilization from fast inactivation in squid giant axons. *Biophys. J.* 54:719–730.

Tanguy, J., and J. Z. Yeh. 1991. BTX modification of Na channels in squid axons. I. State dependence of BTX action. *J. Gen. Physiol.* 97:499–519.

Vandenberg, C., and F. Bezanilla. 1988. Single-channel, macroscopic, and gating currents from Na channels in squid giant axon. *Biophys. J.* 53:226*a*. (Abstr.)

Vandenberg, C., and F. Bezanilla. 1991. A model of sodium channel gating based on single channel, macroscopic ionic, and gating currents in the squid giant axon. *Biophys. J.* 60:1511–1533.